Available online at www.sciencedirect.com

ScienceDirect

Procedia Structural Integrity 12 (2018) 113–121

Structural Integrity Procedia

www.elsevier.com/locate/procedia

AIAS 2018 International Conference on Stress Analysis

Fabrication of fluidic reactors by a customized 3D printing process

Sandro Barone[a], Marcello Braglia[a], Roberto Gabbrielli[a], Salvatore Miceli[a], Paolo Neri[a,*], Alessandro Paoli[a], Armando Viviano Razionale[a]

[a]*University of Pisa. Department of Civil and Industrial Engineering, Mechanical Division. Largo L. Lazzarino 1, 56122 Pisa, Italy*

Abstract

Microfluidic systems demonstrated to improve the analysis of biological and chemical processes by providing a more controlled fluid-handling environment. Typically, microfluidic systems are created in monolithic form by means of microfabrication techniques that constrain designers to work in a two-dimensional space. In this regard, Additive Manufacturing (AM) is a powerful set of technologies that can deal with the complexity of 3D structures producing flow paths with sections differing in size and direction. In this work, the use of a commercial laser-based stereolithography 3D printer has been firstly explored to fabricate transparent channels for flow reactors. A custom 3D printer, based on Digital Light Processing Stereolithography (DLP-SLA), has then been developed with the aim at gaining flexibility and overcoming typical limitations raised from standard commercial solutions. The effectiveness of the developed DLP-SLA 3D printer has been experienced by printing transparent fluidic devices with embedded channels with a specifically designed three-step printing process.

Keywords: Additive manufacturing; fluidic reactor; laser-based stereolithograpy; DLP 3D printing

1. Introduction

The use of microfluidic reactors for flow chemistry in both academic research and industrial applications has considerably grown in the past two decades (Elvira et al., 2013; Waheed et al., 2016). Microfluidics deals with the manipulation and control of fluids geometrically confined into small channels, typically having millimetric scale. The

* Corresponding author. Tel.: +39-050 2218019; fax:+39-050 2218019.
E-mail address: paolo.neri@dici.unipi.it

10.1016/j.prostr.2018.11.102

cross-sectional size of 3D printed fluidic structures can be classified into millifluidic (larger than 1 mm), sub-millifluidic (0.5-1 mm), large microfluidic (100-500 μm) and microfluidic (smaller than 100 μm) (Beauchamp et al., 2017). Most of current microfluidic devices are prepared in a simple planar format in poly-dimethyl-siloxane (PDMS) by soft lithography, a technique based on PDMS micro-molding. PDMS has many outstanding properties for microfluidics since it is optically clear, biocompatible, inert, water impermeable and fairly inexpensive. However, the fabrication process is mainly limited to two-dimensional systems and 3D microfluidics remains a challenge due to the difficulties of producing complex 3D flow paths with sections differing in size and direction.

Additive Manufacturing (AM) is emerging as a novel and powerful set of technologies that can deal with the complexity of real 3D structures. In recent years, the use of AM to create 3D fluidic devices has started to emerge (Capel et al., 2013; He et al., 2016; Yazdi et al., 2016). AM allows to create 3D microstructures with arbitrary geometries and intricate mixing pathways. 3D printing can also simplify the creation of interfaces with the external fluid sources as threaded fittings, or other lock systems, as parts of the fluidic device to guarantee leak-free connections. However, despite the undeniable advancement of AM technologies in the last decade, there are still many challenges that must be faced, which mainly regard the materials (in terms of availability, biocompatibility and colorless transparency), the resolution and the surface roughness.

In the present work, firstly, the use of a commercial solution based on stereolithography to fabricate transparent microchannels for flow reactors has been explored. In particular, the laser-based Formlabs Form2 printer has been used to investigate the possibility to directly print 3D microfluidic devices, at low cost, by changing the way such devices are conceived, designed and manufactured. For example, 3D printing allows the microreactors manufacturing with embedded 3D channels in a single part, without junctions or additional external piping interfaces, which could cause fluid losses. Potentialities and design challenges have been discussed and critical issues have been highlighted. Among these, the most limiting features resulted to be: the surface roughness, which is caused by the deposition of multiple successive layers and by the laser path and affects the optical clarity of the channels; the printer resolution, which impairs the channel size; the trapped resin, which can solidify and block the microchannels.

A custom solution, based on Digital Light Processing Stereolithography (DLP-SLA), has been then developed to overcome the limitations raised from the standard solution. An image can be used to define a mask for each individual layer and projected on the printing plate by using a Digital Micro-mirror Device (DMD), thus allowing a selective photopolymerization of a photosensitive resin. Different layers of the resin are successively exposed to the projector light with appropriate masks to manufacture the entire model. The flexibility of the adopted configuration allows to increase the spatial resolution by varying the projector placement with respect to the resin bath and/or by changing the optical set-up. Moreover, the mechanical system only consists of a single-axis movement instead of a complex laser path definition: each layer is then polymerized all at once, improving the surface smoothness. Finally, the high setup flexibility of a custom solution allows to design ad-hoc printing equipment for the disposal of the trapped resin, thus reducing blocked channel issues and printing direction limitations. The effectiveness of the developed DLP-SLA printer has been finally experienced by printing embedded 3D channels.

2. Laser-based Stereolithography

Most commercially available 3D printers for fluidic applications use one of these three technologies: fused deposition modelling (FDM), polyjet (PJ), or stereolithography (SLA) (Macdonald et al., 2017). FDM uses thermoplastic polymers, as acrylonitrile butadiene styrene (ABS) or polylactic acid (PLA) stored in continuous filaments, which are extruded by a heated nozzle. However, despite their attractive cost with respect to other technologies, they are characterized by a rough surface finish, a non-transparent appearance, and a resolution that is limited by the *xy* plotter, the *z*-stepper motor and the extrusion nozzle diameter (Yazdi et al., 2016). PJ technology uses a sprayer to lay down resin droplets, which are cured by UV light. A sacrificial supporting material is required for embedded voids to allow the successive layer to be deposited on top. In this regard, the effective removal of supporting material from channels represents a critical issue for PJ printed fluidics. SLA exploits a vat of resin that is photopolymerized by a projector or a laser following a predefined path. This technology is particularly suitable for microfluidics since a fluidic device is essentially composed of a series of linked voids within a solid material (Shallan et al., 2014). At the end of the manufacturing process, internal voids contain unpolymerized liquid resin, which can be

removed with an easier process with respect to the removal of supporting materials as required by other 3D printing technologies.

In this work the laser-based SLA Formlabs Form2 has been firstly used to investigate the possibility to directly print 3D microfluidic devices. Commercial SLA printers are characterized by a higher resolution with respect to FDM printers enabling microscale cavity printing. Moreover, the use of proprietary resins, specifically designed to enhance the printing accuracy, allows to outperform the capabilities of the more common ABS and PLA used by FDM printers.

Figure 1(a) shows the CAD model of the designed fluidic device adopted for the fabrication tests. The channels, having section sizes of 2 × 1 mm and 1 × 1 mm, are created within three converging arms, disposed in an arrowhead wise. The viscosity of the resin represents a critical issue in its removal from the channels. The trapped resin could be cured in the UV post-processing, causing blocked channels. For this reason, the orientation of the model within the printing volume has been arranged in order to dispose the smaller channels with the higher slopes, thus facilitating the leakage of the unpolymerized resin during the fabrication process (Fig. 1(b)). Figure 1(b) also shows the supporting structures automatically generated by the PreForm preparation software (Formlabs) before the printing process.

The proprietary photoreactive Clear Resin, which is a mixture of methacrylic acid esters and photoinitiator, has been used to fabricate the fluidic reactor with a slicing resolution of 50 μm. Figure 2(a,b) shows the fabricated fluidic reactor while Figure 2(c) reports an enlargement of the surface roughness obtained by a microscope. Tests demonstrated that channels up to 1 × 1 mm were correctly fabricated. However, the adopted slicing direction on the one hand optimize the leakage of the unpolymerized resin, but on the other further impairs the optical clarity of the device since the multilayer photopolymerization process produces stair steps, which affect the surface roughness. Figure 2(c) highlights the surface signs generated by the layer-by-layer manufacturing that add up to those left by the laser path.

Figure 3(a) shows the results obtained by arranging the model with the slicing direction normal to the arms surface (Fig. 3(b)). This orientation hinders the leakage of the unpolymerized resin from the channels thus causing its further polymerization during the ongoing of the printing process, completely filling the channels as evidenced by Figure 3(a).

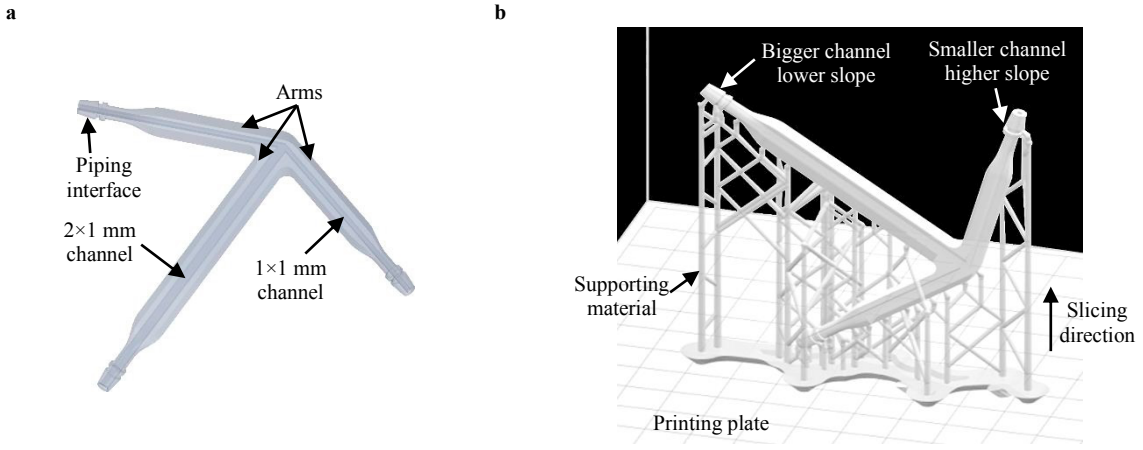

Fig. 1. a) CAD model of the designed fluidic device with internal channels, b) arrangement of the model within the printing volume with the supporting material generated by the preparation software.

a b c

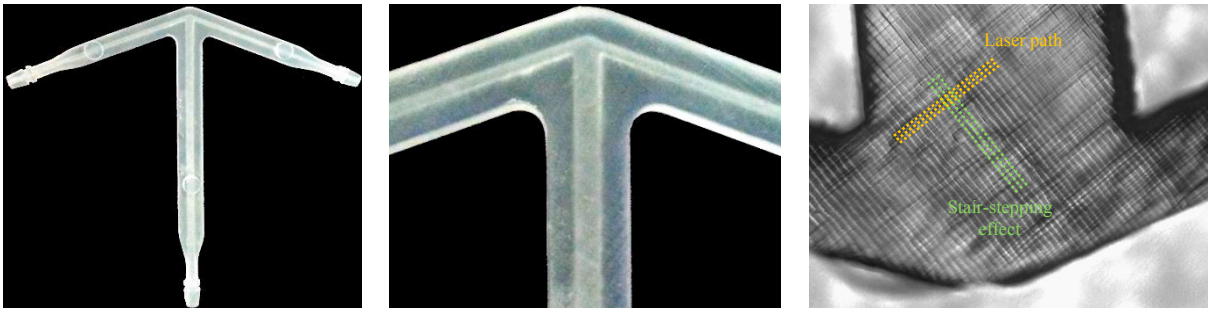

Fig. 2. a) Fluidic device fabricated by using the Formlabs Form 2, b) detail of the mixing area, c) enlargement of the surface finish highlighting two stair patterns: one generated by the laser path during the photopolymerization process, the other by the layer-by-layer additive manufacturing process.

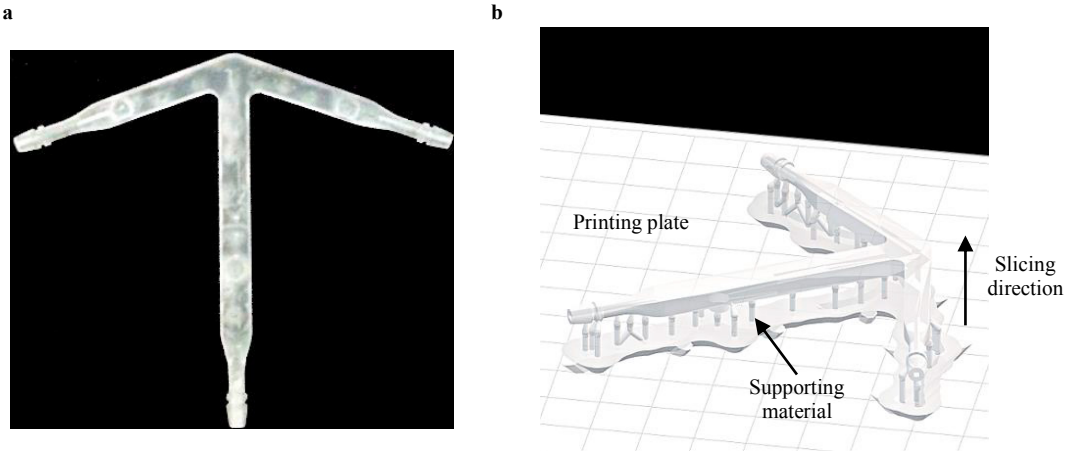

Fig. 3. a) Fluidic device fabricated by using the Formlabs Form 2 with arrangement of the CAD model within the printing volume with a slicing direction normal to the arms surface (b).

3. Development of a custom DLP-SLA printer

The approach proposed in this work relies on the development of a custom 3D printer with the aim at overcoming typical limitations of commercial solutions. The design criteria followed two main requirements: 1) the capability to vary the in-plane (*xy*) resolution, since the void size is constrained by this parameter and 2) the reduction of the moving stages in order to increase dimensional accuracy and surface finish. In this regard, dynamic digital masks for layer-by-layer projection represents a reliable solution, which is faster, cheaper and more robust with respect to vector-operated printers, as only one translational stage (the *z*-axis) is required (Pan et al., 2012). Digital dynamic masks can be generated by using a liquid crystal display (LCD), a spatial light modulator, or a digital micromirror device (DMD) (Gibson et al., 2015). In this work, DMD technology has been used to project spatially resolved patterns through the bottom of a clear resin vat.

3.1. Hardware set-up

The 3D printer (Fig. 4) has been developed by assembling an off-the-shelf DLP projector (OPTOMA EX330e), equipped with a 1024 × 768 micromirror array, a mirror with a tilting axis adjustment, a 3D printing mechanism and a set of custom made mounts (Fig. 4(a)). The use of a commercial projector can significantly reduce the prototype cost simplifying at the same time the system design. The projector is horizontally placed to decrease the vertical height of the printer and fixed to a common base (Fig. 4(b)). The mirror is used to reflect the patterns from the projector and focus them on the bottom of the transparent resin vat. A first surface SiO2-coated aluminum mirror has been used in

order to avoid ghost reflections. The 3D printing mechanism is composed of an aluminum platform, a trapezoidal leadscrew, a flanged leadscrew nut, a stepper motor and two vertical linear guides.

The printing process follows the bottom-up architecture. The image masks are projected on the bottom of the resin vat, while the printing platform moves upward pulling the object out of the resin and allowing the uncured resin to fill the space under the plate created by the polymerized resin. The thickness of each slice is well controlled by the distance between the vat floor and t6he printing plate.

The main advantage of this approach is that it requires only a restricted amount of resin in the vat. On the other hand, the polymerized layer is directly placed on the bottom of the vat, which must then be transparent to the curing wavelength. In this work, a 160 × 190 mm glass vat has been used to guarantee also the surface flatness. Moreover, an anti-sticking solution has been taken into account to prevent the polymerization of the molecules closest to the bottom of the vat and facilitate the lifting to the printing platform. In particular, the bottom of the vat has been covered with a Teflon^{TM} FEP film, which is transparent, inert and characterized by low frictional properties. This film covering needs to be replaced after a certain number of printings.

The printer resolution is strictly related to the hardware setup. The vertical translation of the printing platform is obtained by a flanged nut assembled with a trapezoidal leadscrew, having 2 mm pitch and $l = 8$ mm lead (four starts), and two vertical linear guide rails. A NEMA 17 stepper motor, having a step angle $\theta = 1.8°$, has been used to drive the leadscrew. The theoretical vertical resolution, r_z, can then be obtained as $r_z = l\ \theta / 360°$. A minimum translation value of 0.02 mm is obtained if the half-step mode is used. The horizontal resolution, r_{xy}, is strictly related to the DMD resolution and the size of the projected area. A rectangular projected area of 160 × 120 mm has been defined for a horizontal resolution r_{xy} = 160 mm/1024 pixels ≈ 0.15 mm/pixel. The zoom wheel of the projector lens can be used to further adjust the size of the projected area, thus modifying r_{xy}.

In this work, the Photocentric3D clear DLP UV Firm resin has been used. This resin is a mixture of methacrylate oligomers, methacrylate monomers and photo initiators, and has been specifically designed to work both with 385 nm and 405 nm wavelengths, thus allowing 3D printing process with traditional DLP projectors. Moreover, it exhibits transparency properties, which make it suitable for the fabrication of fluidic channels.

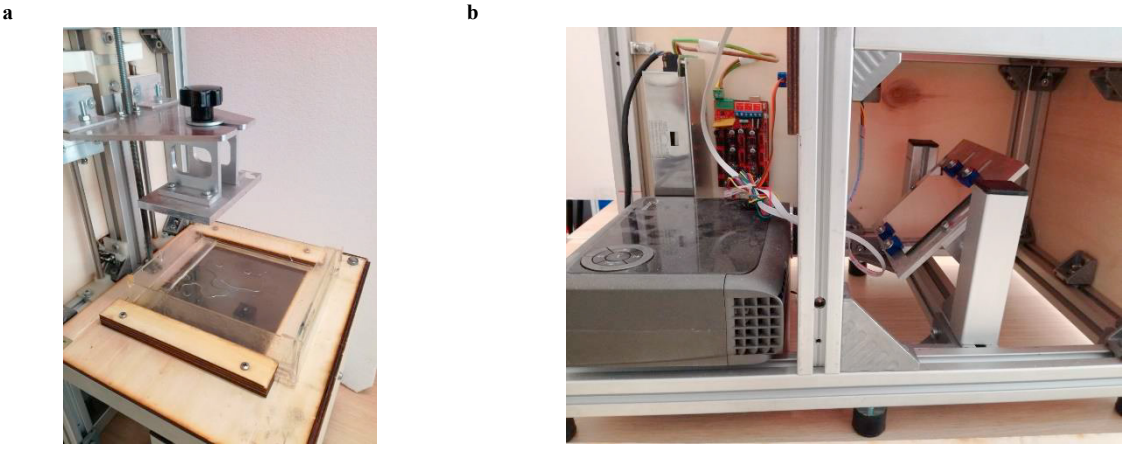

Fig. 4. Assembled DLP-SLA 3D printer. a) Detail of the printing platform and resin vat, b) detail of the light projection system.

3.2. Calibration

Before the printing process, the resin container must be adjusted to be parallel to the printing plate. This task is accomplished by a manual tilting system, arranged with four springs placed at the vat corners. Before the printing stage, the plate is lowered on the bottom of the vat and the springs are used to make the vat surface parallel with respect to the printing plate. Projector settings as focus, keystone distortion, brightness and contrast are adjusted with

the aim at producing a sharp image on the vat surface. The dimensional accuracy is achieved by overlapping a projected calibration grid with a known template.

A specific procedure has been adopted to experimentally evaluate the polymerization thickness, which is a function of the optical dose absorbed by the resin. A plexiglass plate composed of a series of cylindrical hollows (having a diameter of 10 mm, (Fig. 5(a)) is used to define multiple containers, which are filled with a layer of resin of about 6 mm. The containers are then sequentially exposed to a circular pattern, having a diameter of 5 mm, with different exposure times at the maximum light intensity value, resulting in different polymerization depths. The unpolymerized resin is then rinsed with isopropyl alcohol (IPA) and the thickness of the polymerized samples (Fig. 5(b)) are measured with a micrometer screw gauge. This approach allows to obtain a rough estimate of the exposure time that must be used to have a solid, or nearly solid, material of a specific thickness (Fig. 6).

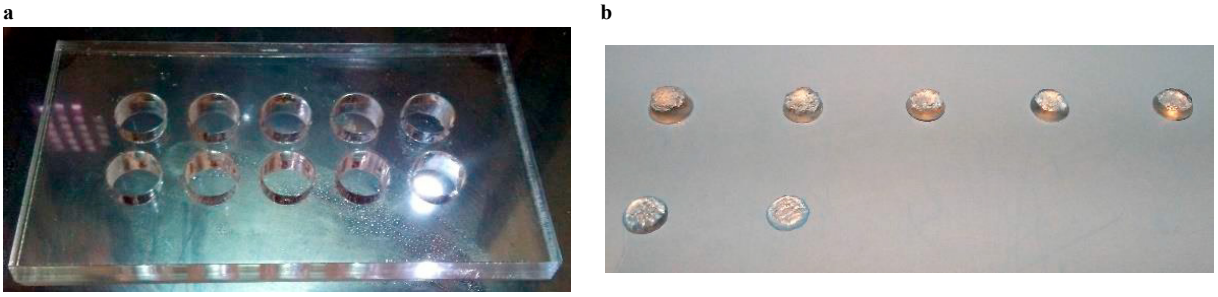

Fig. 5. a) Glass plate with cylindrical hollows, which are filled with resin and sequentially exposed to a circular pattern, b) polymerized samples obtained by using different exposure times

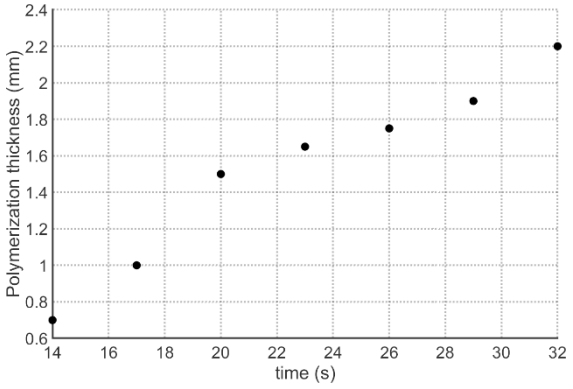

Fig. 6. Polymerization thickness with respect to the exposure time.

4. Microfluidic application

A three-step printing process has been designed to fabricate a transparent fluidic device by using the developed DLP printer. A printing direction perpendicular to the arrow surface is selected to avoid the stair-stepping effect on the top surface. The unpolymerized resin, which remains within the channels during the printing process, affects the results since its overexposure during the printing process of the top layers leads to the channels blockage. For this reason, the fluidic reactor has been virtually divided in two distinct parts: the base part, composed of the bottom layers and the channel layer, and the top part, composed of a single layer making the channel ceiling (Fig. 7). A layer thickness of 1 mm was set for the overall printing process due to the constraint imposed by the channel height (1 mm). The first printing step consists in producing the base part on the printing plate with a conventional printing procedure (Fig. 7(a-c)). Then the printing plate is lifted at a safe height, avoiding the risk that further illumination could

polymerize the residual resin, occluding the channels. The second printing step is then carried out by projecting on the bottom of the resin tank the image corresponding to the top part (Fig. 7(d-f)). This procedure allows to polymerize a region, attached to the tank, having the shape of the top part, and a height depending on the exposure time. A polymerization height of 1 mm was assured by using an exposure time of about 17 s (Fig. 6). Once polymerized the top parts, it is then possible to lower the printing plate (holding the base part) on to the top part (Fig. 7(g-i)). The cohesion between base and top parts is achieved by projecting once again the image corresponding to the channel layer. In this way, only the resin laying outside the channels is exposed to this latter illumination, thus avoiding channels occlusion. At the end of the process, the distinction between base and top parts is not visible anymore, since the last polymerization step perfectly bonded the interface region (Fig. 7(i)). The printed channels are finally syringed with isopropyl alcohol to rinse the unpolymerized resin and cured with a UV post processing

Figures 7(i) and 8(a) show two examples of the results obtained with non-occluded channels having minimum size of 2 × 1 mm and 1 × 1 mm, respectively. Also, since the layer thickness was set to 1 mm (requiring an exposure time of about 17 s per layer), the overall 3D printing process required less than 2 minutes. Figure 8(b) reports an enlargement, detailing the surface roughness, obtained by a microscope. The comparison with Fig. 2(c) proves the effectiveness of the proposed approach in the manufacturing of void channels without any texture on the surface, thus enhancing the surface finish and, consequently, the optical clarity.

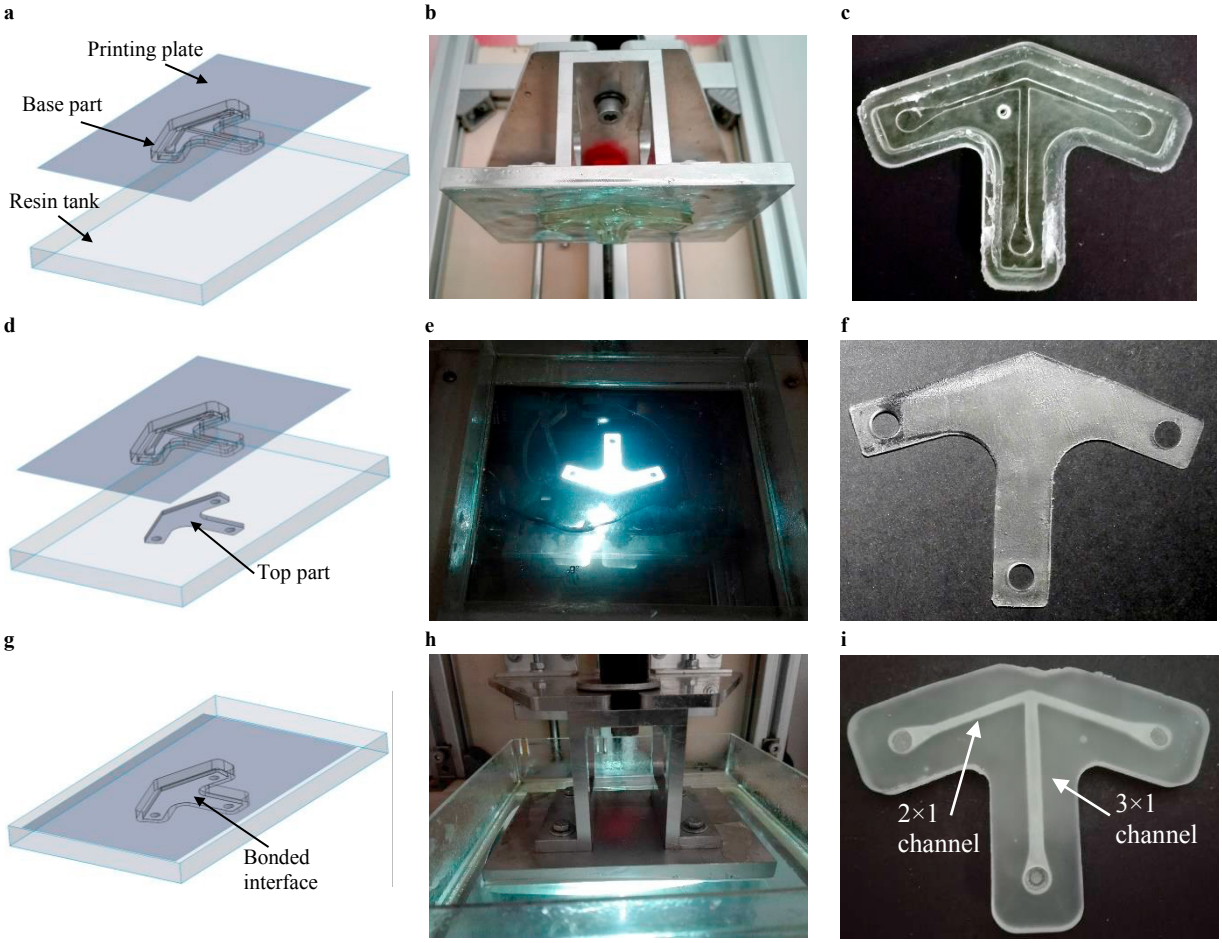

Fig. 7. Three-step printing process of fluidic devices. a) Scheme of the first step, which consists in the base part printing, b) lifting of the printing plate with the base part attached on it, c) fabricated base part, d) scheme of the second step, which consists in the top part printing, e) polymerization of the top part on the bottom of the resin tank, f) fabricated top part, g) scheme of the third step, which consists in the integration between the two parts, h) lowering of the printing plate and last polymerization phase, i) fabricated fluidic device characterized by a minimum channel size of 2 × 1 mm.

Fig. 8. a) Transparent fluidic device fabricated by using the developed DLP-SLA 3D printer and characterized by a minimum channel size of 1 × 1 mm, b) enlargement of the mixing area that highlights the surface finish, and thus the improved optical clarity, with respect to Fig. 2(c).

5. Discussion and conclusions

Additive manufacturing based on stereolithography allows for the fabrication of completely encapsulated 3D fluidic channels. However, one of the most limiting peculiarities of AM technologies is the restricted choice of materials available for the fabrication of functional devices. Moreover, the high cost of commercial 3D printers hinders their flexibility since the use of non-proprietary materials may violate warranty conditions. Significant further concerns are represented by the prevention of channel blockage, due to the over exposure of the resin during the manufacturing, and the surface finish, which is affected by the stair-stepping effect typical of layer-based processes and impairs the optical clarity. These issues heavily constrain the overall design of the printing process and affect the quality of the final product. For all these reasons, a custom DLP-SLA printer has been developed by exploiting an off-the-shelf projector. The overall setup introduces a high flexibility in the design of the printing process as demonstrated by the non-conventional three-step procedure developed for the fabrication of transparent fluidic devices with embedded channels.

The 3D printing process is a trade-off between resolution, processing time and final model size. High-resolution systems can be usually obtained only for small working volumes. The proposed solution does not represent an exception since the working distance of the DLP projector can be varied thus modifying both resolution and printing size. However, projectors with a greater resolution could be used allowing to print smaller features without modifying the designed setup. Furthermore, the integration between a custom 3D printer and a specifically-designed resin could greatly increase the complexity of the manufacturable shapes (Gong et al., 2017). The developed 3D printer, indeed, could be further customized by substituting the DLP projector with a LED projection system with a spectrum tailored to take advantage of the specific resin.

Acknowledgements

The authors are grateful to the University of Pisa for supporting this research activity (Grant: PRA_2017_49).

References

Beauchamp, M.J., Nordin, G.P., Woolley, A.T., 2017. Moving from millifluidic to truly microfluidic sub-100-mu m cross-section 3D printed devices. Anal Bioanal Chem 409, 4311-4319.

Capel, A.J., Edmondson, S., Christie, S.D.R., Goodridge, R.D., Bibb, R.J., Thurstans, M., 2013. Design and additive manufacture for flow chemistry. Lab Chip 13, 4583-4590.

Elvira, K.S., Solvas, X.C.I., Wootton, R.C.R., deMello, A.J., 2013. The past, present and potential for microfluidic reactor technology in chemical synthesis. Nat Chem 5, 905-915.

Gibson, I., Rosen, D.W., Stucker, B., 2015. Additive manufacturing technologies: 3D printing, rapid prototyping and direct digital manufacturing, Second edition. ed. Springer, New York, NY.

Gong, H., Bickham, B.P., Woolley, A.T., Nordin, G.P., 2017. Custom 3D printer and resin for 18 mu m x 20 mu m microfluidic flow channels. Lab Chip 17, 2899-2909.

He, Y., Wu, Y., Fu, J.Z., Gao, Q., Qiu, J.J., 2016. Developments of 3D Printing Microfluidics and Applications in Chemistry and Biology: a Review. Electroanal 28, 1658-1678.

Macdonald, N.P., Cabot, J.M., Smejkal, P., Guijt, R.M., Paull, B., Breadmore, M.C., 2017. Comparing Microfluidic Performance of Three-Dimensional (3D) Printing Platforms. Anal Chem 89, 3858-3866.

Pan, Y., Zhao, X., Zhou, C., Chen, Y., 2012. Smooth surface fabrication in mask projection based stereolithography. Journal of Manufacturing Processes 14, 460-470.

Shallan, A.I., Smejkal, P., Corban, M., Guijt, R.M., Breadmore, M.C., 2014. Cost-Effective Three-Dimensional Printing of Visibly Transparent Microchips within Minutes. Anal Chem 86, 3124-3130.

Waheed, S., Cabot, J.M., Macdonald, N.P., Lewis, T., Guijt, R.M., Paull, B., Breadmore, M.C., 2016. 3D printed microfluidic devices: enablers and barriers. Lab Chip 16, 1993-2013.

Yazdi, A.A., Popma, A., Wong, W., Nguyen, T., Pan, Y.Y., Xu, J., 2016. 3D printing: an emerging tool for novel microfluidics and lab-on-a-chip applications. Microfluid Nanofluid 20.